JOURNAL OF GEOPHYSICAL RESEARCH, VOL. 103, NO. D15, PAGES 19,149–19,159, AUGUST 20, 1998

Nitric oxide production by simulated lightning: Dependence on current, energy, and pressure

Y. Wang, A. W. DeSilva, and G. C. Goldenbaum

Department of Physics and Institute for Plasma Research, University of Maryland, College Park

R. R. Dickerson

Department of Meteorology, University of Maryland, College Park

Abstract. The production of NO has been studied by means of arc discharges in the laboratory which simulate natural lightning in current waveform and amplitude ($\simeq$ 30 kA). Observations are compared to the results of a computational model that includes the dynamics of energy deposition and channel expansion, combined with the Zel'dovich equations to model the relevant chemical reactions. Results are expressed as NO produced per meter of arc length, and are measured as functions of dissipated energy and of peak current. It is found that at atmospheric pressure, the NO production per joule of dissipated energy is not constant. NO production per meter discharge length as a function of peak current appears to provide a more appropriate scaling factor for estimates of total global NO production. Production of NO_2 was less than 10% of the production of NO, and by implication the production of O_3 less still. From these data, and using published estimates of global lightning frequency, we derive an estimate of global NO production of 2.5 Tg(N)/yr for 30 flashes per second to 8.3 Tg(N)/yr for 100 flashes per second.

1. Introduction

Nitric oxide plays an important role in atmospheric photochemistry and in global biogeochemical cycles and hence is an essential part of the determination of global climate [*Crutzen,* 1973; *Price et al.,* 1997]. In 1857 von Liebig suggested that lightning could fix atmospheric nitrogen that eventually was washed from the atmosphere as nitrate in rainwater. In more recent times, *Noxon* [1976] measured the NO_2 below a thunderstorm and found more fixed nitrogen than in the surroundings. Estimates of the rate of NO production vary widely [e.g., *Lawrence et al.,* 1995]. Theoretical estimates have been determined; field and laboratory experiments have been performed.

Measurements of NO production in controlled laboratory conditions are important for an understanding of the physical and chemical processes involved. Issues that need to be investigated include whether heating in the expanding shock wave is sufficient to produce significant NO [*Tuck,* 1976], or whether it is produced mostly in the central current-carrying channel, which we refer to as the "core" [*Hill,* 1979; *Hill et al.,* 1980], or in the surrounding corona sheath. Also, what determines the amount of NO that remains in the atmosphere? The usual way of looking at this is to consider a rapid initial heating to a high temperature (e.g., 20,000 K) followed by rapid cooling [*Zel'dovich and Raizer,* 1966]. At temperatures above about 2500 K the chemical reaction rates for producing and destroying NO are sufficiently rapid that the NO density is the equilibrium value for the instantaneous temperature. As the temperature rapidly drops below this value, the reaction rates become so small that the NO destruction processes cannot keep up with the falling temperature and the density of NO is "frozen" at the higher temperature [e.g., *Chameides et al.,* 1977]. Details of the specific physical processes involved are poorly understood. For example, is the limiting balance of production and decay determined by the heating rate, hydrodynamic expansion, turbulence, instability, molecular thermal loss processes, or something else? Additional questions on relating the amount of NO produced to simple scaling laws need to be answered if global estimates on NO production are to be simply made.

A widely used figure of merit is the amount of NO produced per joule of energy. It is usually assumed that this figure of merit is a constant. Since the production rate depends on the local and instantaneous thermal and flow parameters, a more complete understanding of how energy is dissipated is necessary to validate the use of such a figure of merit to make estimates of global NO production by lightning. Because of the complexity of the phenomena involved, these questions cannot now be simply answered by observations of natural light-

Paper number 98JD01356.
0148-0227/98/98JD-01356$09.00

ning. Recent laboratory experiments [*Stark et al.*, 1996] have investigated some of these questions. In particular they found that shock heating is ineffective for producing NO_x, implying that all production is from the core behind the shock. They also claimed to have directly measured the freeze-out mixing ratio.

We studied the production of NO in laboratory discharges designed to simulate the physics and chemistry occurring in natural lightning. This means making arc discharges in air, having current profiles that have time history and amplitude as similar as possible to those of natural lightning. The results reported here represent a compromise between achieving short risetimes and high current with the apparatus available. Discharges are made in a closed chamber, in which the pressure may be varied to simulate atmospheric conditions from sea level up to 8 km. The amplitude of the current was also varied from 5 to 30 kA. In this experiment, peak current occurs at 30 μs. In natural lightning the time to peak varies widely, with a mean time to peak of 5 μs [*Price et al.*, 1997].

In addition, we have modified a numerical model previously reported by *Goldenbaum and Dickerson* [1993] and compare experimental results with the model. The model contains the time- and space-dependent physics of energy deposition, the subsequent dynamics associated with the expansion and shock wave of the arc channel, and the chemistry of the Zel'dovich reactions responsible for formation of NO. Our intention is to develop an understanding of the processes involved by comparing model results initially with the laboratory experiment and eventually with natural lightning. The present results represent our attempt at defining useful operational parameters for future detailed measurements.

2. Experiment

The arcs simulating natural lightning are struck between 5 cm diameter hemispherical electrodes in a cylindrical stainless steel chamber measuring 1 m in length and 1 m in diameter, fitted with 66 cm long by 45 cm diameter coaxial extensions (Figure 1). The electrodes protrude in from the ends and are tipped with Elkonite, a copper-tungsten sinter having excellent spark erosion resistance.

In natural lightning a low-current leader ionizes a small channel that the main current stroke follows. Similarly in the experiment, a short (submicrosecond) voltage pulse from a 250 kV Marx high-voltage generator produces the leader (Figure 2). This pulse can form an arc up to 20 cm in length in 1 atm pressure air. The main high-current discharge, having peak current up to 30 kA, is supplied by a capacitor bank having capacitance $C = 1035$ μF (the "main bank"), charged to 5–10 kV. This bank is isolated from the Marx generator by a spark gap switch. It is necessary to isolate this low-voltage bank from the Marx generator to avoid short-circuiting the high-voltage pulse into the low impedance of the main bank. The isolating switch is filled with SF_6, pressurized to about 2 atm. It is fired after the leader discharge, and it closes about 80 μs after the leader discharge, sending the main current pulse into the channel formed by the leader. Considerable recombination of the leader channel occurs during this interval, so the gap must be made smaller than 20 cm if the main bank is to discharge. At full atmospheric pressure the arc gap must be set to 4 cm or less in order for the main bank discharge to take place. At lower pressures the gap may be larger.

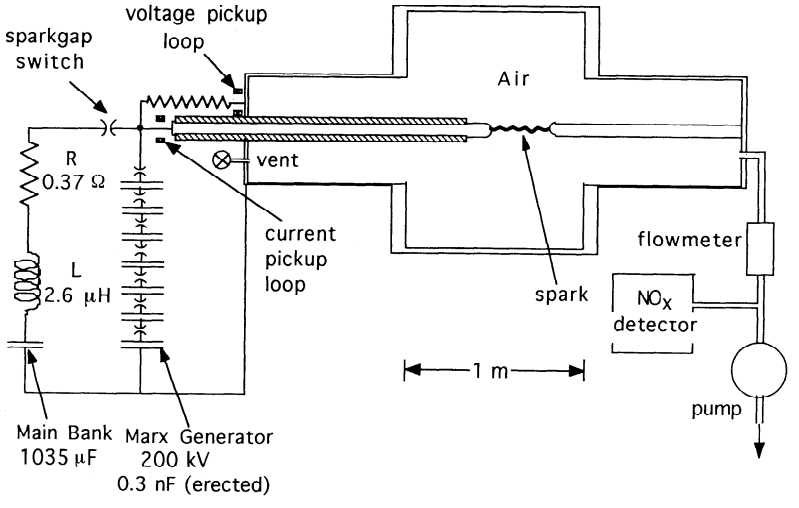

Figure 1. Schematic of experiment. Spark occurs between a high-voltage electrode and a grounded electrode in the center of the chamber. The NO detector samples a small fraction of the gas stream as it is pumped out of the chamber, while ambient air enters through the vent. The energy storage capacitor is rated at 18 kV, but used at less than 10 kV.

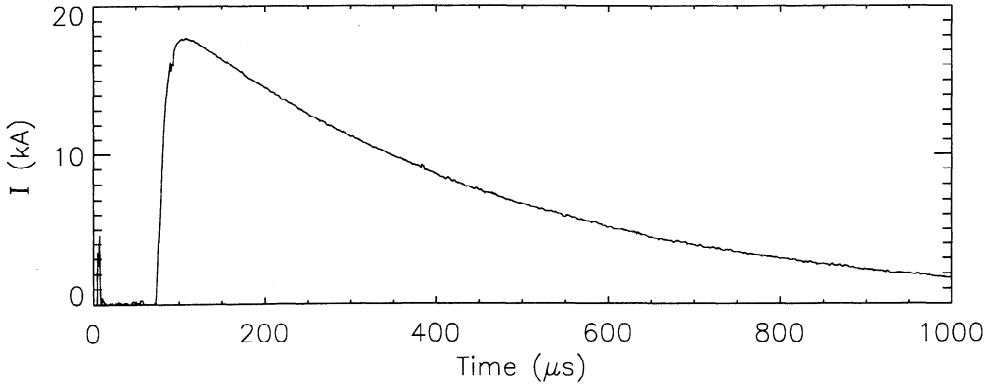

Figure 2. Current waveform. The spike at $t = 0$ represents the Marx discharge.

The inductance of the main bank and associated cables that conduct current to the electrodes is $L = 2.6\ \mu$H. In addition to the pressurized switch, the main bank has a 0.37 Ω resistor, R, in series, which gives the desired risetimes and decay times to simulate natural lightning. The risetime is determined roughly by L/R, and the decay time by RC. With this resistor the current rises to a peak in about 30 μs, and decays over about 400 μs (Figure 2). The impedance of the spark is sufficiently small compared to the external impedance that the waveform is almost independent of charge voltage, gap length, or ambient pressure.

3. Diagnostics

The voltage across the arc gap is measured by means of a resistive voltage divider, and the current derivative is measured with a pickup loop (Figure 1). The pulsed voltage $V(t)$ measured by the divider is the sum of an inductive part LdI/dt and the resistive part IR_a, which is responsible for energy deposition in the channel. Net energy input as a function of time is given by

$$U(t) = \int_0^t V(t')I(t')dt'. \quad (1)$$

Substituting for V the inductive and resistive contributions, we have

$$U(t) = \int_0^t I^2(t')R_a(t')dt' - \frac{L}{2}\int_0^t I\,\frac{dI}{dt'}dt'. \quad (2)$$

When the integration extends to infinity, the last term is automatically zero, since the current is zero at both limits, and we find that the net resistive energy deposition into the spark is given simply by the integral of (1), taken with the upper limit infinity. In practice, the experimentally observed signals are integrated until the inductive term is no more than 1% of the resistive term.

We have photographed the arc using two instruments. A rotating mirror streak camera with Polaroid™ type 667 film was used to record the expansion of the channel in visible light. For this measurement the center of the arc was imaged onto a narrow slit oriented at a right angle to the arc axis. Light passing through this slit was swept by a rotating mirror and reimaged onto the photographic film, producing a light image for which one dimension is radius and the other time. From such an image, one may determine the growth of the channel radius. Second, the structure of the discharge was photographed at several times after initiation of the main discharge with a short-exposure (e.g., 5 ns) electronic camera having an S20 spectral response ($\sim$ 380 nm–700 nm).

Following each discharge, the air in the chamber is exhausted by a pump. A mass flow meter measures dm/dt, the rate at which mass is discharged, and a chemiluminescent NO analyzer samples the gas to determine the mixing ratios f(NO) and f(NO_x). The mass flow rate and mixing ratio are recorded until the fraction of NO falls to $< 1\%$ of its maximum. The total mass of NO produced in the arc is then computed from

$$m_{NO} = \int_0^\infty f\frac{dm}{dt}dt. \quad (3)$$

To calibrate the detector, a bottle containing 1.32 ± 0.012 ppm of NO in N_2 was prepared and calibrated by the National Institute of Standards and Technology (NIST). The detector was then checked against this calibrated mix. The flow meter accuracy is estimated to be $\pm 2\%$. The largest source of error in determination of NO content is in precision of the NO measurement, estimated to be ± 5–10%.

4. Simulation

The numerical model integrates the hydrodynamic and chemical reaction rate equations (see *Goldenbaum and Dickerson* [1993] and references therein). That paper assumed an instantaneous energy deposition in a cylindrical core. The model used here assumes that energy is deposited by Ohmic heating arising from a current that reaches a peak value of typically 5 to 30 kA in 30 μs and decays with a decay time constant of about 400 μs. The model used for conductivity includes a combination of elastic and ionizing electron-neutral and collective electron-ion collisions [*Braginskii*, 1965].

For this purpose the column is divided into cylindrical annuli, with the conductivity in each annulus being determined by the local temperature and density. The specific energy rate equation then contains a source term $\sigma E^2/\rho$, where ρ is the mass density, σ the conductivity, and E the electric field. The electric field is determined by estimating the admittance for the entire column as a summation over all annuli and assuming Ohm's law,

$$E(t) = \frac{I(t)}{\sum_i \sigma_i \pi (r_i^2 - r_{i-1}^2)}. \quad (4)$$

Energy losses include radiative and ionization losses. The radiative losses are treated in an approximate manner using a combination of atomic spectral line and bremsstrahlung continuum radiation. For the early time results reported here the radiation losses did not appear to be important. The calculation assumes collisions are sufficiently frequent that all species have the same temperature and that energy is equilibrated among the vibrational, rotational, and translational degrees of freedom. The calculation is intended to model the main discharge, that is, the return stroke. As such, it starts with assumed parameters in a cylindrical core meant to represent the conditions after the Marx discharge, that is, the leader. These conditions in natural lightning as well as this experiment are not well understood at this time. It is found that the parameter that most affects the outcome is the initial core radius. At the present time we only know the core size as observed in visible light, while the relevant size is the diameter of the current channel. In addition, the model cannot account for instabilities or turbulence that have been observed in other experiments late in the discharge [*Picone et al.*, 1981].

5. Experimental Results

We have measured both the NO and NO_x content of the air after a discharge with a chemiluminescent detector, having a 375° Mo converter calibrated with gas-phase titration [e.g., *Dickerson et al.*, 1995]. We found that in all cases the NO_x fraction is only about 5-10% greater than the NO fraction. On a given shot, over 95% of the stored energy in the main capacitor bank is dissipated in the external 0.37 Ω resistor, and only a small fraction is actually dissipated in the air spark. In natural lightning cloud, undisturbed air and ground resistance also dissipate energy. It is not possible at this time to unequivocally determine the fraction of stored energy that is dissipated in natural lightning. For this reason we plot in Figure 3 the NO production as a function of the energy dissipated in the spark, as given by (1) above. As has been observed elsewhere, the amount of NO produced increases with energy. This could be due to several effects, including higher temperature, an increase in turbulence, or an increase in spark diameter. The results of the measurements of NO per meter versus dissipated energy per meter displayed in Figure 3 are quite scattered. A linear least squares fit to these data gives

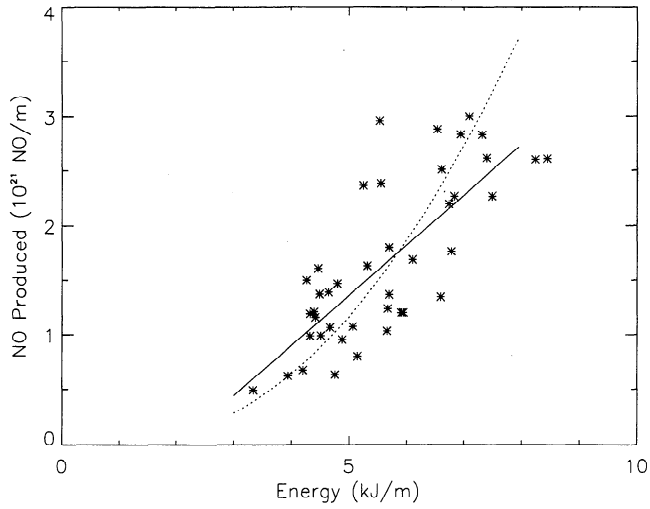

Figure 3. NO production as a function of dissipated energy in a spark, normalized to 1 m spark length. The solid line is a linear least squares fit to the data. The dotted line is a quadratic representation derived from fits in Figures 4 and 5.

$$n_{NO}(W) = a + bW, \quad (5)$$

where $a = -0.94 \pm 0.35$, $b = 0.46 \pm 0.06$, with W in kJ/m and n_{NO} in units of 10^{21} NO/m. The correlation coefficient $r^2 = 0.59$, which reflects the poor correlation of the fitted curve with the data. The standard deviation of individual shot data from regression is $\pm 0.48 \times 10^{21}$ NO/m.

Although the scatter in the data of Figure 3 do not justify making a quadratic fit in (5), we find using the same data set that there is a reasonably good correlation between the amount of NO/m produced and the peak current. Figure 4 shows this relation, along with the least squares quadratic fit .

$$n_{NO}(I) = a + bI + cI^2, \quad (6)$$

where I represents peak current amplitude, $a = 0.14 \pm 0.33$, $b = 0.026 \pm 0.036$, and $c = 0.0025 \pm 0.0009$. The multiple correlation coefficient $r^2 = 0.89$, and the standard deviation from regression is 0.25×10^{21} NO/m.

From the same data set, the relation between peak current and dissipated energy also shows relatively little scatter (Figure 5), and may be fit reasonably well by the relation

$$W(I) = a + bI, \quad (7)$$

where W is in kJ/m, I is again kA, and $a = 2.31 \pm 0.41$, $b = 0.17 \pm 0.02$, $r^2 = 0.72$, and the standard deviation is 0.74 kJ/m. The true relation $W(I)$ must go to zero as I goes to zero, but in the range for which we have data, a linear fit is adequate. Since both the fits of (6) and (7) have relatively high confidence levels, they may

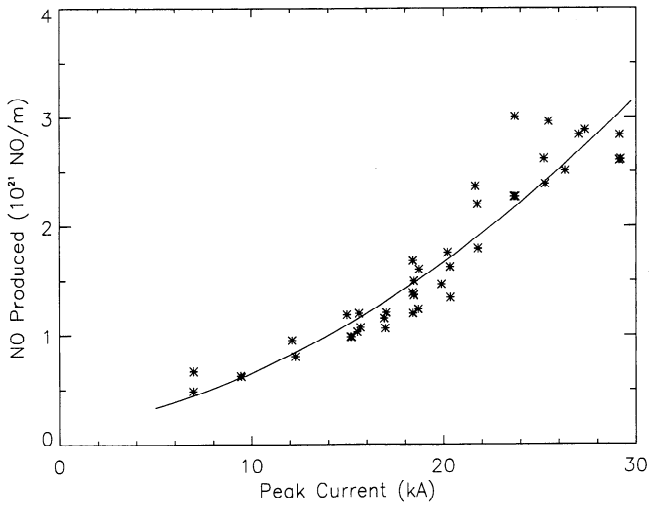

Figure 4. NO production normalized to 1 m spark length, as a function of maximum current in the spark, at 1 atm pressure, $T = 20°$ C.

be combined to give a quadratic relation that improves on (5) and which represents our best approximation to the data of Figure 3:

$$n_{NO}(W) = a + bW + cW^2, \tag{8}$$

where $a = 0.251 \pm 0.65$, $b = -0.245 \pm 0.29$, and $c = 0.0857 \pm 0.038$. This quadratic approximation is included in Figure 3 as a dotted line.

Using fast-exposure (5 ns) photography, we have seen that on some shots the arc is a single channel, while occasionally (approximately one shot in 10) a forked or double channel forms. Consequently, some of the variation in the data may be due to the occasional occurrence of such anomalous discharges.

The production rate has also been measured as a function of the air pressure at constant initial temperature (293 K), from 10^5 Pa down to about 3×10^4 Pa.

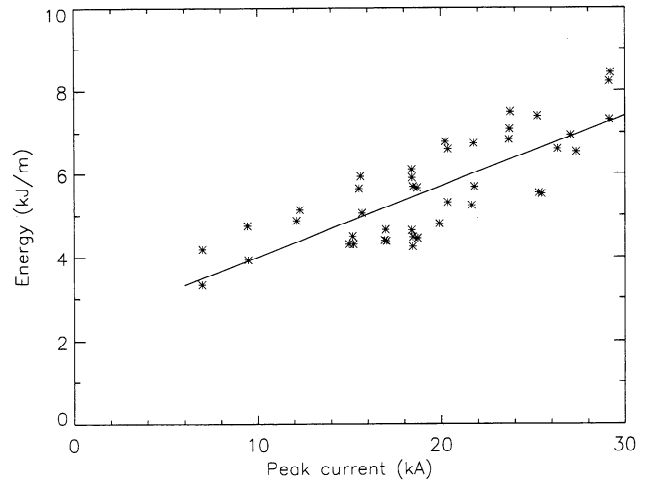

Figure 5. Energy dissipated as a function of peak current for the same data set in Figures 4 and 3.

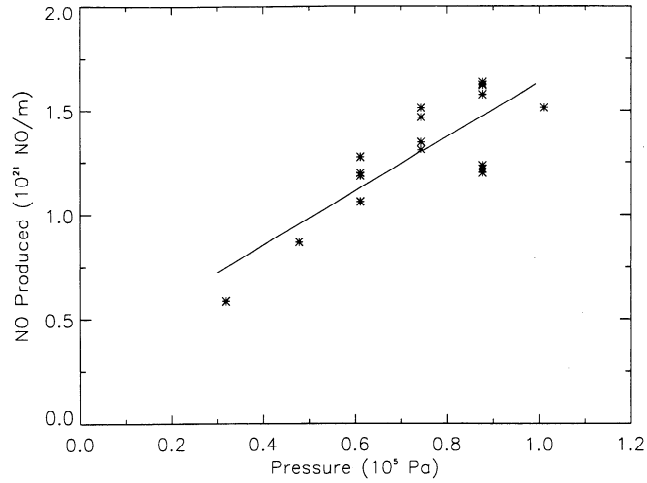

Figure 6. Variation of NO production per meter with initial air pressure in chamber (gap 3.2 cm, peak current 19 kA).

This corresponds to varying density from ground level to about 8 km. For this measurement the chamber was pumped down to the desired pressure, the discharge was fired, and then the chamber was filled with air and the NO measurement was made as previously discussed. Results are shown in Figure 6 for a peak current of 19 kA. Over this range of pressures the mass of NO produced is practically linearly proportional to the initial laboratory air pressure. With p in pascals (1 atm = 1.01×10^5 Pa) and n_{NO} in 10^{21} molecules per meter,

$$n_{NO}(p) = a + bp, \tag{9}$$

where $a = 0.34 \pm 0.18$, $b = 1.30 \pm 0.23$, and $r^2 = 0.67$.

We are concerned about the possibility of end effects near the electrodes contributing significantly to the measured resistance. The electric sheath at the ends

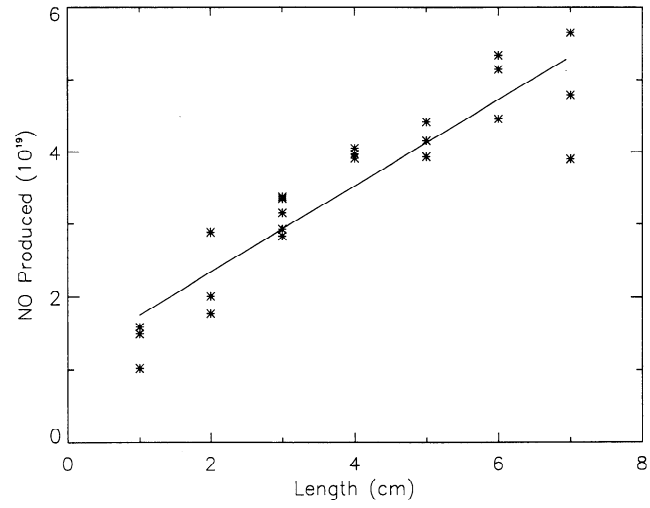

Figure 7. Sensitivity of NO production to length of spark gap, at a pressure of 342 mbar and peak current 19 kA.

is expected to have a thickness of the order of the Debye length [*Chen*, 1984], which for our conditions is less than 1 μm, and should therefore have little effect. Also, the voltage drop across the sheath should be no more than a few kT/e, which is only about 1% of the net resistive drop. The effect of thermal conduction is to cool the plasma in the vicinity of the electrodes. This process is described by a diffusion equation, in which the scale length for the temperature gradient is proportional to the square root of the time over which diffusion occurs. Inserting appropriate parameters for the thermal conductivity of a plasma at 10,000 K [*Spitzer*, 1967], at the initial atmospheric density, one finds that the gradient scale length is about 0.15 mm after 10 μs, and about 0.5 mm after 100 μs. The scale length has only a very weak dependence on assumed density, and varies as the 5/4 power of temperature. We conclude that thermal conduction cooling to the electrodes may be neglected. Sputtering of electrode material into the arc is a possibility, which we minimize through use of low-sputtering materials.

An experimental approach to determination of the influence of end effects is to change the arc length, holding all other parameters constant, and to measure NO production. We have done this at a pressure of 0.34×10^5 Pa, for which successful discharges may be made with electrode spacing up to 6 cm. Figure 7 shows the NO production for several electrode spacings. The production of NO tends to a value only slightly greater than zero as the gap length tends to zero, suggesting that there is some end influence that tends to increase NO production in the vicinity of the electrodes. Correction for the amount of additional NO produced seems unwarranted when compared to the shot-to-shot variability.

6. Simulation Results

The simulation has been compared with the experiment for a variety of conditions. The simulation has been run using the measured current waveform in the experiment with different leader core parameters. It should be emphasized that the simulation is only capable of describing the early time dynamics phase. Because the simulation is one dimensional it will not properly simulate long-term effects such as turbulent heating or cooling. For a fixed core radius there is little dependence of amount of NO produced on the initial densities of the minor constituents (electrons, NO, N, and O). The amount of NO produced depends mainly on the initial radius of the core, that is, the region of elevated temperature (taken to be 500 K) and electron density (typically 10^{14} to 10^{16} cm^{-3}) in which the current is initially largest. For a radius of 1.0 cm and 20 kA peak current the simulation predicts about $n_{NO} \approx 1 \times 10^{21}$ molecules/m, which is approximately what the experiment gives.

In the experiment the amount of NO increases with peak current. This is not reproduced in the simulation, if the initial core radius is maintained constant. The only experimental measurement of the initial core radius is by visible light photography, which shows an initial radius of about 0.5 cm. Until further measurements more completely specify the initial conditions, the computed amount of NO will remain uncertain. On the other hand, the present simulation can be a guide to the time sequence of events during the early energy deposition phase which are qualitatively the same for a variety of reasonable initial conditions.

The time dependence of the total number of NO molecules produced shows a rise to a saturation value.

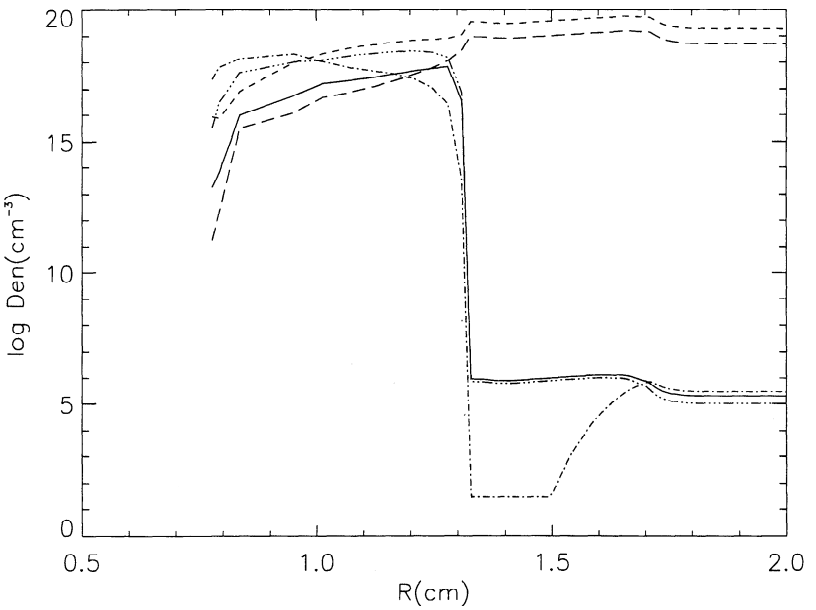

Figure 8. Simulation code result at 14 μs for a 20 kA discharge. Shown are radial plots of the log of the density (in cm^{-3}) for different chemical species: short-dashed curve, N_2; long-dashed curve, O_2; dash-dotted curve, N; dash-tripple-dot curve, O; and solid curve, NO.

In the simulations the time to reach saturation depends on current amplitude for a fixed core radius. In Figure 8 we show the radial dependence of the densities of N_2, O_2, NO, N, and O and in Figures 9 and 10 we show the temperature, pressure, and mass density at one particular time in a 20 kA discharge. This is typical of all times after the total amount of NO produced has become approximately constant. In Figure 8 the shock front is at $r = 1.75$ cm and the outer edge of the core is at $r = 1.32$ cm. It is clear in the simulation that most of the NO is produced in the core region far behind the shock wave. This is because only in this region is the temperature sufficiently high for a significantly high reaction rate. Notice that at $r = 1.0$ cm the N_2 and O_2 densities are less than 10% of their ambient values. The fact that the temperature is highest in the low-density, evacuated core is consistent with the previous simulations of *Plooster* [1971] and *Paxton et al.* [1986]. Looking at the radial plots in Figure 8, we can understand the sequence of events in producing NO. As the shock wave moves into the ambient air (300 K), a small amount of heating occurs, producing an order of magnitude increase in NO at the expense of N. Some of the rise in NO density is due to chemical reactions and some is due to compression. At smaller radii the temperature rises significantly due to Ohmic heating in the evacuated low-density region (Figure 9). At this point a large increase in the NO density occurs in a narrow region. (The thickness of this transition may be greater due to turbulence and viscous effects not included in the model.) At the same time as the core is expanding, resulting in a drop in density, dissociation of O_2 and N_2 occurs. The reduction in O_2 and N_2 results in a lower reaction rate for the reactions producing NO. Since expansion lowers all the densities, both the forward and backward reaction rates will be affected. Expansion also has an effect on the temperature because the dissipated energy is shared by fewer particles. However, the heating rate is complicated by the dependence of conductivity on both temperature and density, leading to a nonlinear dependence of the temperature on the density decrease.

In an effort to separate the hydrodynamics from the chemistry we ran the code with the Ohmic heating but with the dynamics turned off, resulting in spatial uniformity of all quantities. The time variation of the various quantities is shown in Figure 11. It is apparent that at early times (< 1.1 μs) NO is produced by the reaction

$$N + O_2 \longrightarrow NO + O. \tag{10}$$

As the concentration of O increases, at some point NO production is enhanced by the other Zel'dovich reaction

$$O + N_2 \longrightarrow NO + N. \tag{11}$$

The NO concentration is rapidly increased until at about 2.5 μs, dissociation decreases the O_2 concentration, thereby effectively shutting off the first reaction and decreasing the NO production rate. In the simulations with hydrodynamics included, expansion reduces the O_2 concentration faster than dissociation and is thus the limiting factor. It should also be noted that during hydrodynamic expansion the overall density decreases while the dissipation continues depositing energy into fewer particles, resulting in higher temperatures than in the constant density simulation.

Another factor arising from the full simulation as well as the partial simulation, which complicates the interpretation of scaling parameters, is the fact that the limiting NO concentration is reached before peak current. Hence the scaling of NO with energy or current has more to do with the rate of increase of current, or

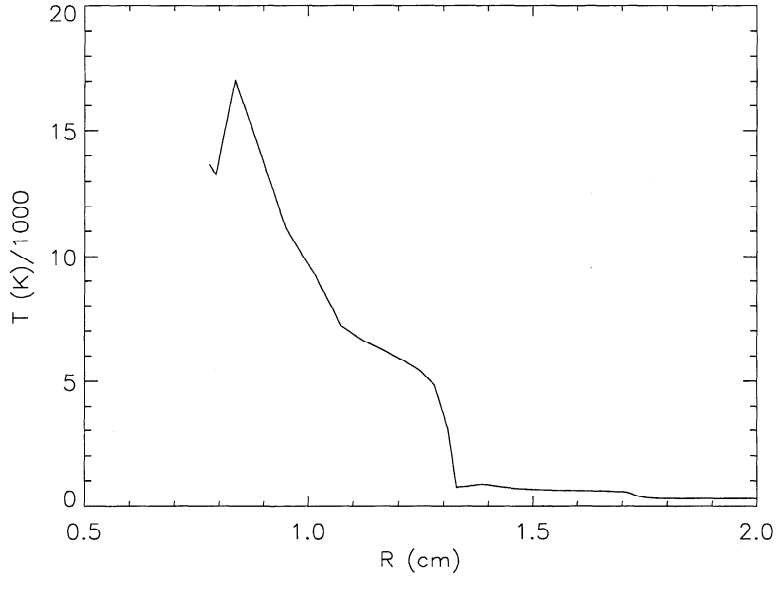

Figure 9. Simulation code result of the temperature for the same case as shown in Figure 8.

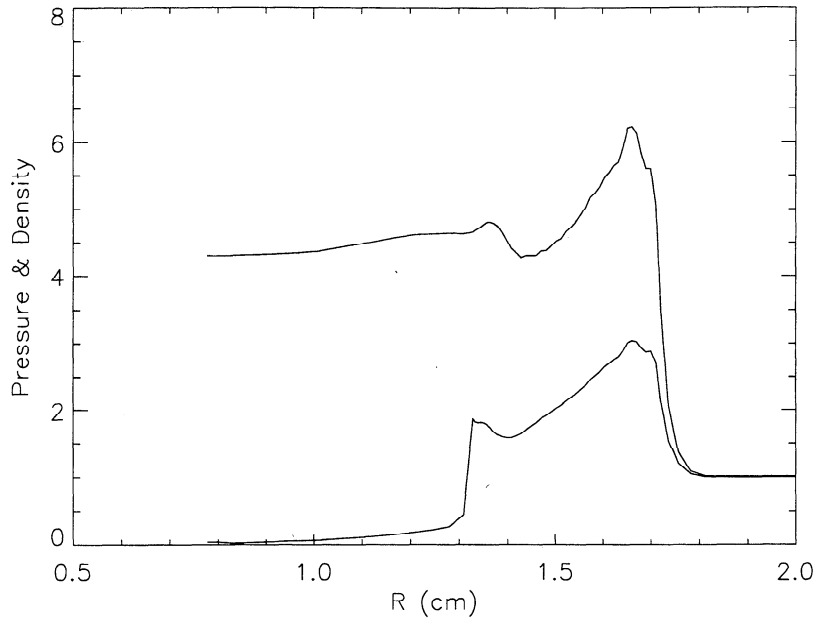

Figure 10. Simulation code results for the normalized pressure (top curve) and mass density (bottom curve) for the same case as Figure 8.

the power dissipated, than with the amplitude. This is not unexpected if one considers the spark channel as a chemical reactor. Power is input through Ohmic heating. The power primarily divides among heat, radiation, and mass motion. The mass motion results in an increase of the reactor volume, reducing the density of reactants. Since there is no further input of reactants, the output shuts off.

The simulation is incapable of describing the possible later time turbulent mixing of cold ambient atmosphere into the hot, low-density core. Because of this, the simulation cannot say anything about the importance of the freeze-in effect in determining the eventual amount of NO.

7. Calculations of Global NO From Lightning

The contribution of lightning to the global reactive nitrogen budget has been the subject of much research and speculation. Several methods have been employed, but an accurate assessment requires evaluation of

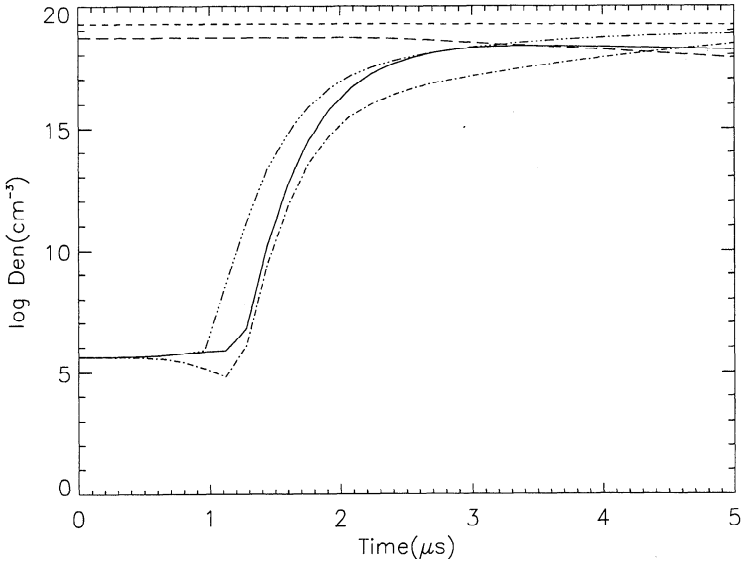

Figure 11. Simulation code results at constant density with the hydrodynamics turned off but with the same time dependence of the current as Figures 8–10. The notation for the chemical species is the same as in Figure 8.

several difficult to estimate variables. In this section we estimate the global production of NO based on our experimental results. The results presented here are focused on cloud-to-ground flashes. Intracloud flashes are more frequent, but generally thought to be less energetic and shorter than cloud-to-ground flashes [*Krehbiel*, 1986; *Lawrence et al.*, 1995; *Price et al.*, 1997]. *Cooray* [1997] and *Gallardo and Cooray* [1996] estimated that equivalent amounts of energy are dissipated by intracloud and cloud-to-ground flashes. Despite the pressure effect predicted by *Goldenbaum and Dickerson* [1993] and demonstrated experimentally here, results from a recent field experiment suggest that intracloud flashes can not be neglected. Measurements from a high altitude aircraft indicate substantial NO production from intracloud flashes in three storms over the Great Plains [*Stith*, 1998]. Because of the great uncertainty surrounding intracloud flashes we limit our estimate to NO produced from cloud-to-ground flashes.

The most frequently used method of calculating the global NO production is what *Lawrence et al.* [1995] referred to as the flash extrapolation approach (FEA), in which the total global NO production is estimated from

$$G(\mathrm{NO}) = P(\mathrm{NO})F_f, \tag{12}$$

where $P(\mathrm{NO})$ is the number of molecules of NO produced by a typical single lightning flash and F_f is the global annual lightning flash frequency. The value of $P(\mathrm{NO})$ has been estimated from field observations of natural lightning [*Noxon*, 1976, 1978; *Drapcho et al.*, 1983; *Franzblau and Popp*, 1989] and from laboratory discharges [*Chameides et al.*, 1977; *Levine et al.*, 1981]. NO produced by laboratory discharges must be somehow extrapolated to properties of natural lightning. This extrapolation often has been made with the efficiency of NO production per joule of energy $p(\mathrm{NO})$ as the parameter. Results presented here, however, indicate that this parameter may be inappropriate for global estimates. As suggested by *Chameides* [1986, 1979], $p(\mathrm{NO})$ appears to vary. Our laboratory measurements indicate that this is not a constant, that is, that there is not a simple proportionality between energy dissipated and NO production. Referring to Figure 3, the data are rather scattered, but a simple proportionality seems clearly excluded. This conclusion is further illustrated in Figure 12 where we plot $p(\mathrm{NO})$ as a function of peak current.

For currents typical of lightning the values of $p(\mathrm{NO})$ obtained are considerably higher than previous measurements. For example, *Hill et al.* [1988] measured NO production in a much lower current (70 mA), lower energy (5.7 mJ) device and found $p(\mathrm{NO}) = 1.4\times10^{16}$ NO/J. *Levine et al.* [1981] have utilized a higher-energy device (12 kJ). The current magnitude and waveform were not specified so it is not possible to compare their results with ours. Using the stored energy their results yield $5 \pm 2 \times 10^{16}$ NO/J. *Chameides et al.* [1977] measured the NO produced using a 35 kV electrostatic generator connected in parallel to a 59 pF capacitor. The stored energy in each cycle was 36×10^{-3} J. The current magnitude and waveform were not reported. Using stored energy, without attempting to correct for other circuit losses, they estimated the figure of merit as $6 \pm 1 \times 10^{16}$ NO/J. Moving their detector to larger energy storage device (1350 J) they obtained one shot from which they estimate $p(\mathrm{NO}) = 8 \times 10^{16}$ NO/J. Because of the difficulty in producing large amplitude, fast risetime currents, we suspect all of these experiments had currents considerably smaller than ours. It is noteworthy that extrapolating the curve in Figure 12 to low energies (and hence low currents) gives values not dissimilar to the previous results.

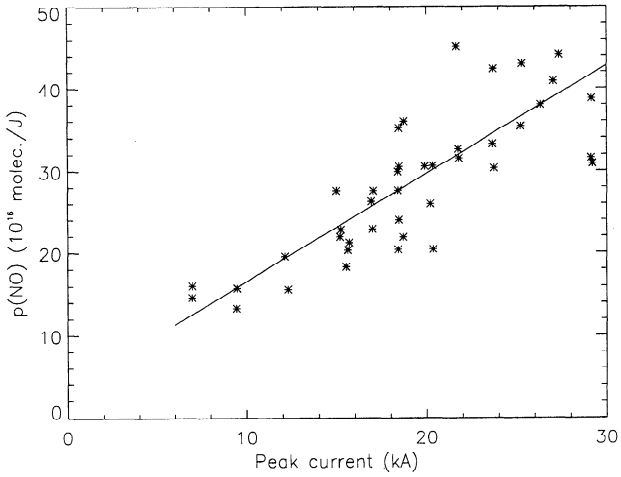

Figure 12. NO production divided by the energy dissipated, $p(\mathrm{NO})$, as a function of peak current.

The fraction of stored atmospheric electrical energy that goes into NO production, into the Earth's surface, and into the cloud itself are all highly uncertain. Using a new approach, *Price et al.* [1997] multiplied the atmospheric breakdown potential (about 3×10^8 V) by the cloud charge necessary to produce a maximum current of 36 kA, the mean peak current measured over the United States [*Orville*, 1991a,b]. They derived an average energy of about 6 GJ per flash. The resistance of the atmosphere, however, falls after the passage of the leader, and the lightning voltage probably decreases substantially in the course of the flash. We believe that the value of 6 GJ is an upper limit, and the actual values for energy released into the atmosphere by lightning lie well below this. Other investigators have estimated 0.4 GJ per flash (see *Lawrence et al.* [1995] for a review). The relationship of (7) implies that over this range of data the perturbed atmosphere is not simply a constant resistance resistor. Extrapolating to the mean current of 36 kA [*Price et al.*, 1997], the mean energy dissipated per unit length is 8.4 kJ/m. For a 6 km altitude cloud with a tortuosity factor of 3.6 (see discussion in the next paragraph) and assuming 2.8 strokes per flash with the

second and subsequent strokes having current at 43% of the initial stroke [*Price et al.*, 1997], this results in an energy dissipation of 0.37 GJ/flash.

If the peak current in natural lightning is much better known than the energy dissipated, as implied by *Orville* [1991b], then using the NO produced per unit length as a function of pressure and peak current may be a more reliable means of estimating the production per flash. To model the troposphere, we assume the undisturbed atmosphere to be an ideal gas with a linear lapse rate $B = 6.5 \times 10^{-3}$ K/m. Integration of (9) along the path of length H leads to the number of NO molecules (in units of 10^{21} molecules) produced per stroke as

$$N_{NO} = -0.533\,H + 4.12 \times 10^{-5} \frac{P_0 T_{lab}}{B\delta}(1 - A^{\delta}) - 2.08 \times 10^{-10} \frac{(P_0 T_{lab})^2}{T_0 B(2\delta - 1)}(1 - A^{2\delta - 1}) \quad (13)$$

where $T_0 = 288$ K is the model atmosphere temperature at ground level, $P_0 = 1 \times 10^5$ Pa is the model atmospheric pressure at ground level, $T_{lab} = 294$ K is the laboratory temperature at which the measurements leading to (9) were made, $H = 6000$ m, a typical cloud altitude, $\delta = g/RB$, $g = 9.8 m/s^2$, $R = 287$ J kg^{-1}K^{-1} and $A = 1 - BH/T_0 = 0.865$. Modifying the coefficients of (9) for 36 kA by multiplying by the ratio $n_{NO}(36\,\text{kA})/n_{NO}(19\,\text{kA})$ of the number of molecules per meter obtained from (6), we obtain a value of 2.1×10^{25} molecules for each 36 kA stroke. In order to account for the NO produced in multiple stroke flashes, we make use of the multiplicity (strokes per flash) versus frequency (flashes per minute) plot (Figure 2b in the paper by *Price et al.* [1997]). Using this scatterplot we estimate an average of 2.8 strokes per flash. In order to estimate the efficiency of NO production by multiple strokes, we use *Price et al.*'s [1997] observation that second and subsequent strokes on average have peak currents of 43% of that of the primary stroke. Taking all of this into account we find 3.1×10^{25} molecules per flash. Assuming 30 [*Price et al.*, 1997] to 100 [*Lawrence et al.*, 1995] flashes per second, we estimate 0.7 Tg(N)/yr for 30 flashes per second and 2.3 Tg(N)/yr for 100 flashes per second.

The experimental results we report here are for discharges considerably shorter in length than a typical cloud altitude. In order to apply these results, we need to account for the tortuous path of the natural lightning discharge. Although some observational data exist [*Hill*, 1968], it is difficult to use in estimating the altitude multiplication factor ((H_{total}/H) = tortuosity). We will estimate this factor using a theoretical model based on a random walk of constant step length between fixed endpoints. The step size is determined by the leader discharge and has been estimated to have a representative length $\langle h \rangle = 50$ m [*Uman*, 1982]. This length is sufficiently long as not to be a factor in the laboratory experiment. The tortuosity is estimated by the relation $H_{total}/H \approx (H/\langle h \rangle)^{D-1}$, where D is the fractal dimension [*Vecchi et al.*, 1994; *Valdiva*, 1997]. The fractal dimension for a lightning discharge has been estimated by *Vecchi et al.* [1994] as 1.2 for a step length of 35 m and 1.5 for 90 m. Choosing D= 1.27, and H= 6000 m, we find a tortuosity factor of 3.6. If we assume a multiplication of the path length due to tortuosity of 3.6, then these estimates grow to 2.5 and 8.3 Tg(N)/yr. Due to the uncertainties associated with the flash rate and tortuosity in the above calculation, we have not made a correction for the 5-10% NO_2 production. There are additional uncertainties associated with applying our experimental results to natural lightning, both known, such as the effect of current risetime, and unknown. These uncertainties can only be quantified through additional measurements leading to a better understanding of the discharge physics.

Acknowledgments. This work was supported by the NSF (grant ATM9408179), and will form a part of the Ph.D. thesis of Yu-Jin Wang. We are indebted to H.-J. Kunze for his careful reading of the manuscript and comments.

References

Borucki, W. J., and W. L. Chameides, Lightning: Estimates of the rate of energy dissipation and nitrogen fixation, *Rev. Geophys., 22*, 363-372, 1984.

Braginskii, S. I., Transport processes in a plasma, in *Reviews of Plasma Physics, vol. 1*, edited by M. A. Leontovich, p. 221, Consultants Bureau, New York, 1965.

Chameides, W. L., Effects of variable energy input on nitrogen fixation in instantaneous linear discharges, *Nature, 277*, 123-125, 1979.

Chameides, W. L., The role of lightning in the chemistry of the atmosphere, in *The Earth's Electrical Environment*, pp. 70-77, Natl. Acad. Press, Washington, D.C., 1986.

Chameides, W. L., D. H. Stedman, R. R. Dickerson, D. W. Rusch and R. J. Cicerone, NO_x production in lightning, *J. Atmos. Sci., 34*, 143-149, 1977.

Chen, F. F., *Introduction to Plasma Physics and Controlled Fusion, vol. 1: Plasma Physics*, p. 8, Plenum, New York, 1984.

Cooray, V., Energy dissipation in lightning flashes, *J. Geophys. Res., 102*, 21401-21410, 1997.

Crutzen, P. J., A discussion of the chemistry of some minor constituents in the stratosphere and troposphere, *Pure Appl. Geophys., 106*, 1385-1399, 1973.

Dickerson, R. R., B. G. Doddridge, P. K. Kelley, K. P. Rhoads, Large-scale pollution of the atmosphere over the North Atlantic Ocean: Evidence from Bermuda, *J. Geophys. Res., 100*, 8945-8952, 1995.

Drapcho, D. L., D. Sisterson, and R. Kumar, Nitrogen fixation by lightning in a thunderstorm, *Atmos. Environ., 17*, 729-734, 1983.

Franzblau, E., and C. J. Popp, Nitrogen oxides produced from lightning, *J. Geophys. Res., 94*, 11089-11104, 1989.

Gallardo, L., and V. Cooray, Could cloud to cloud discharges be as effective as cloud to ground discharges in producing NO_x?, *Tellus, 48B*, 641-651, 1996.

Goldenbaum, G. C., and R. R. Dickerson, Nitric oxide production by lightning discharges, *J. Geophys. Res., 98*, 18,333-18,338, 1993.

Hill, R. D., Analysis of irregular paths of lightning channels, *J. Geophys. Res. 73*, 1897-1906, 1968.

Hill, R. D., On the production of nitric oxide by lightning, *Geophys. Res. Lett., 6,* 945-947, 1979.

Hill, R. D., R. G. Rinker, and H. D. Wilson, Atmospheric nitrogen fixation by lightning, *J. Atmos. Sci., 37,* 179-192, 1980.

Hill, R. D., I. Rahmin, and R. G. Rinker, Experimental study of the production of NO, N_2O, and O_3 in a simulated atmospheric corona, *Ind. Eng. Chem. Res., 27,* 1264-1269, 1988.

Krehbiel, P. R., The electrical structure of thunderstorms, in *The Earth's Electrical Environment,* pp. 90-113, Nat. Acad. Press, Washington, D.C., 1986.

Lawrence, M. G., W. L. Chameides, P. S. Kasibhatla, H. Levy, II, and W. Moxim, Lightning and atmospheric chemistry: The rate of atmospheric NO production, in *Handbook of Atmospheric Electrodynamics,* vol. 1, edited by H. Volland, pp. 189-202, CRC Press, Boca Raton, Fla., 1995.

Levine, J. S., R. W. Rogowski, G. L. Gregory, W. E. Howell, and J. Fishman, Simultaneous measurements of NO_x, NO, and O_3 production in a laboratory discharge: Atmospheric implications, *Geophys. Res. Lett., 8,* 357-359, 1981.

Noxon, J. F., Atmospheric nitrogen fixation by lightning, *Geophys. Res. Lett., 3,* 463-465, 1976.

Noxon, J. F., Tropospheric NO_2, *J. Geophys. Res., 83,* 3051-3057, 1978.

Orville, R. E., Lightning ground flash density in the contiguous United States - 1989, *Mon. Weather Rev., 119,* 573-577, 1991a.

Orville, R. E., Calibration of a magnetic direction finding network using measured triggered lightning return stroke peak currents, *J. Geophys. Res., 96,* 17,135-17,142, 1991b.

Paxton, A. H., R. L. Gardner, and L. Baker, Lightning return strokes. A numerical calculation of the optical radiation, *Phys. Fluids, 29,* 2736-2741, 1986.

Picone, J. M., J. P. Boris, J. R. Greig, M. Raleigh, and R. F. Fernsler, Convective cooling of lightning channels, *J. Atmos. Sci., 38,* 2056-2062, 1981.

Plooster, M. N., Numerical simulation of spark discharges in air, *Phys. Fluids, 14,* 2111-2123, 1971.

Price, C., J. Penner, and M. Prather, NO_x from lightning, 1, Global distribution based on lightning physics, *J. Geophys. Res., 102,* 5929-5941, 1997.

Spitzer, L., *Physics of Fully Ionized Gases, 2nd ed.,* p. 144, Wiley-Interscience, New York, 1967.

Stark, M. S., J. T. H. Harrison, and C. Anastasi, Formation of nitrogen oxides by electrical discharges and implications for atmospheric lightning, *J. Geophys. Res., 101,* 6963-6969, 1996.

Tuck, A. F., Production of nitrogen oxides by lightning discharges, *Q. J. R. Meteorol. Soc., 102,* 749-755, 1976.

Uman, M. A., *Lightning,* p. 4, Dover, New York, 1982.

Valdiva, J. A., The physics of high altitude lightning, Ph.D. dissertation, Univ. of Md., College Park, 1997.

Vecchi, G., D. Labate, and F. Canavero, Fractal approach to lightning radiation on a tortuous channel, *Radio Sci., 29,* 691-704, 1994.

Zel'dovich, Y. B., and Y. P. Raizer, *Physics of Shock Waves and High Temperature Hydrodynamic Phenomena,* vol. 1, edited by W. D. Hayes and R. F. Probstein, Academic, San Diego, Calif., 1966.

A. W. DeSilva, G. C. Goldenbaum, and Y. Wang, Department of Physics and Institute for Plasma Research, University of Maryland, College Park, MD 20742-3511. (e-mail: desilva@glue.umd.edu; ggoldenb@dcans.umd.edu)

R. R. Dickerson, Department of Meteorology, University of Maryland, College Park, MD 20742-2425. (e-mail: russ@atmos.umd.edu)

(Received January 20, 1998; revised March 20, 1998; accepted April 17, 1998.)